Mapping indicators of lake ecology at Lake Starnberg, Germany – First results of Sentinel-2A

Katja Dörnhöfer(1), Peter Gege(2), Bringfried Pflug(3) , Natascha Oppelt(1),

(1)Kiel University, Department of Geography, Ludewig-Meyn-Str.14, 24098 Kiel (Germany)
Email:doernhoefer@geographie.uni-kiel.de, oppelt@geographie.uni-kiel.de
(2)German Aerospace Center, Remote Sensing Technology Institute, Oberpfaffenhofen, 82234Weßling (Germany)
Email:peter.gege@dlr.de
(3)German Aerospace Center, Remote Sensing Technology Institute, Rutherfordstr. 2, 12489 Berlin-Adlershof (Germany), Email: bringfried.pflug@dlr.de

ABSTRACT

With the advent of Sentinel-2A new, unprecedented opportunities emerged for analyzing lakes by remote sensing with respect to spatial, radiometric, spectral and temporal resolution. This study is based on a Sentinel-2A scene acquired at Lake Starnberg, an oligotrophic, peri-alpine lake. Atmospheric correction with Sen2Cor worked well showing, however, a small overcorrection in some bands. The lake was analyzed with WASI-2D for suspended particulate matter (SPM) and absorption by coloured dissolved organic matter ($a_{CDOM(440)}$) in optically deep water; in optically shallow, water bottom coverages and water depths were retrieved in addition. Compared to in situ measurements, SPM was overestimated whereas $a_{CDOM(440)}$ agreed well. Water depths estimation performed reasonably up to measured Secchi depth (RMSE: 0.42 m).

1. INTRODUCTION

Lakes represent important ecosystems which offer a variety of ecosystem services [1]. Several stressors such as climate change, eutrophication, morphological alterations and contaminations, however, threaten their ecological functions [2]. To address these threats various national (e.g. US Clean Water Act) and international (e.g. European Water Framework Directive) legislations exist which include regular monitoring of water bodies [3]. Optical remote sensing can assist to obtain indicators of lake ecology including chlorophyll-a (chl-a), suspended particulate matter (SPM), coloured dissolved organic matter (CDOM); in shallow water bottom coverage and water depths can be retrieved as well [4]. Sentinel-2 offers great potential to investigate and monitor indicators of lake ecology at spatial and temporal scales which traditional point based in situ samplings are unable to cover. Sentinel-2 is therefore expected to have a high potential for deriving information on optically active water constituents and shallow water benthos.

This study focused on Lake Starnberg, a deep, oligotrophic, peri-alpine lake. Earlier studies at Lake Starnberg used airborne hyperspectral data to derive water depths [5] or macrophytes and water constituents [6]. Reference [7] used multispectral RapideEye data to map invasive macrophytes [7]. Our study aimed to test Sentinel-2A (S-2A) data for their suitability for estimating water constituents, shallow water bottom coverage and water depth. For the entire processing we used freely available software. We applied Sen2Cor atmospheric correction [8] and the Water Colour Simulator WASI-2D [9] for analyzing the water body. In situ measured reflectance spectra and water samples enabled an evaluation of modelling results.

2. METHODOLOGY

2.1. Study area and in situ data

Lake Starnberg is a 56.4 km² large, peri-alpine lake located in southern Bavaria, Germany (11°19'14'' E, 47°49'34'' N, Fig. 1). The lake is up to 127.8 m deep (average depth: 53.2 m) and developed during the last ice age. Relative to the lake's volume the catchment (314.7 km²) is small and is predominated by forests and cultivated grasslands. The inflow consists of few small creeks and groundwater resulting in a long residence time of water (21 years). The outflow, the river Würm, is located in the North [10]. Since the 1970s, lake restoration programmes such as the construction of a circular sewer line system reduced a former eutrophic development. Currently, its trophic state is classified as oligotrophic [11].

On August 13th 2015, radiance reflectance measurements above the water surface were conducted with an Ibsen spectroradiometer (390-850 nm, 0.5 nm sampling interval) concurrently to a S-2A overpass (-1 and +2 hours). Measured Secchi depth was in average 4.2 m (±0.3 m). On the day before, water samples were collected at the same locations (Fig. 1) and analyzed in a laboratory for a_{CDOM}, chl-a and SPM concentrations. For a_{CDOM} estimation, water samples were filtered through a Whatman GF/F filter (pore size 0.7 µm). The filtrates were measured photometrically with a Perkin Elmer Lambda 1050 spectrophotometer according to [12]. SPM was determined gravimetrically by filtering water (1 l) through pre-weighed cellulose-acetate filters (pore size 0.45 µm). After drying at 105°C filters were weighed again to retrieve SPM concentration by subtraction (cf. [13]). For chl-a, water (1 l) was filtered through GF/F filters (pore size 0.7 µm); pigments were extracted with acetone (99.9 %) and analyzed by high performance liquid chromatography.

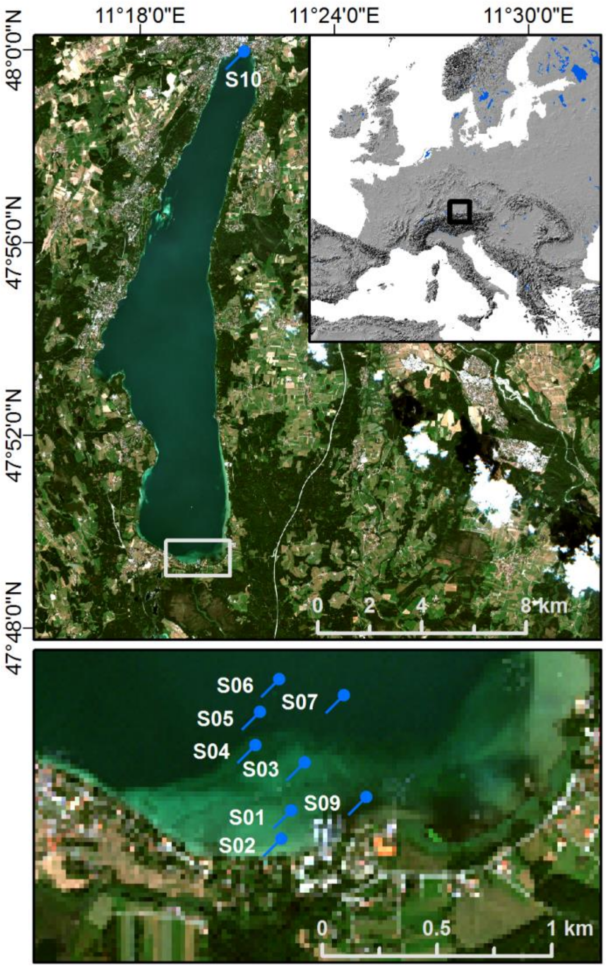

Figure 1. S-2A true-colour composite (20 m) of the study area and location of measurement points.

2.2. Preprocessing of Sentinel-2A data

S-2A acquired a scene of Lake Starnberg on August 13th, 2015 at 12:16 (UTC+2). Atmospheric correction of reprocessed pre-operational L1C Sentinel-2A data (processing baseline 02.01) was conducted with Sen2Cor (Version 2.0.6, [8]). Tab. 3 lists parameters which were used for atmospheric correction. For assessing vertical water vapour column and aerosol optical thickness (AOT) Sen2Cor uses S-2A bands B8a and B9 resp. B2, B4 and B12.

Table 1. Viewing and sun angles over Lake Starnberg during S-2A image acquisition.

	Sun zenith	Sun azimuth	Viewing zenith	Viewing azimuth
Min	35.53°	153.53°	7.86°	99.37°
Max	35.68°	153.72°	8.39°	109.33°

Lacking a correction of water surface effects Sen2Cor calculates bottom of atmosphere (BOA) irradiance reflectance above water ($R(0^+)$). We then applied Eq. 1 to convert $R(0^+)$ into remote sensing reflectance $R_{rs}(0^+)$

$$R_{rs}(0^+)\ [sr^{-1}] = R(0^+)/(10\,000 \cdot \pi) \qquad (1)$$

To evaluate the performance of the atmospheric correction we calculated S-2A $R_{rs}(0^+)$ mean spectra and standard deviations from a 3x3 pixel environment surrounding each of the in situ measurement points. We averaged measurements of each measurement point, convoluted them with the Sentinel-2A spectral response curves and compared the mean values with the satellite spectra. The correlation coefficient (R) and Root Mean Square Error (RMSE) served as performance indicators. R indicates the correspondence in shape whereas RMSE gives the absolute difference between reflectance spectra [14].

To distinguish between water and land we applied the modified normalised water index [15] using the S-2A bands B3 (560 nm) and B12 (2190 nm). Optically deep and shallow water were separated according to the official 8 m bathymetry line [16].

2.3. Parameterization of WASI-2D

WASI-2D is a software tool for analyzing remote sensing imagery by spectral inversion and optimization [9], downloadable from [17]. WASI-2D inversely models R_{rs} spectra by means of radiative transfer. The optimization approach varies fit parameters such as water constituents and water depths within a pre-defined range until measured and modelled spectra achieve the best match (residuum < 1.0E-4). In case of a non-optimal match WASI-2D stops further iterations at a pre-defined maximum number. For modelling $R_{rs}(0^+)$ in optically deep and shallow water we used the R_{rs} model of [18]. Conversion between Sen2Cor $R(0^+)$ and $R_{rs}(0^+)$ followed Eq. 1.

S-2A bands B2 (490 nm), B3 (560 nm), B4 (665 nm) and B5 (705 nm) were the input for inverse modelling in shallow water; B6 (740 nm) and B7 (783 nm) were additionally used in deep water. We therefore resampled the WASI spectral database to the spectral response curves of S-2A [19]. In optically deep water, SPM, $a_{CDOM(440)}$ and the sun glint factor g_{dd} were fit parameters. Scattering by SPM was considered as wavelength-independent with the WASI default backscattering coefficient (0.0086 m^2g^{-1}).

Dinoflagellates were chosen as phytoplankton type using the specific absorption coefficient from the WASI-2D data base. a_{CDOM} predominates absorption processes at Lake Starnberg [5]. Since both chl-a and CDOM strongly absorb in the blue wavelength region [20], and the atmospherically corrected dataset currently offers only one band in this wavelength region (see also section 3.1), fitting both constituents may lead to ambiguous modelling results, in particular if concentrations are low. Therefore, chl-a concentration

was kept constant (0.8 µgl^{-1}oriented at in situ measurement values) in both optically deep and shallow water.
In optically shallow water, the sun glint factor was fixed at -0.01. During inverse modelling, the negative value slightly alleviates overcorrection of $R_{rs}(0^+)$ spectra by Sen2Cor. SPM, $a_{CDOM(440)}$, water depths and bottom coverage (sediments and macrophytes) were considered as fit parameters. To estimate the latter, WASI-2D requires irradiance reflectance spectra of sediment resp. macrophytes as model input. The macrophyte spectrum (*Chara contraria*) originated from the WASI spectral database; the sediment spectrum was measured ex situ in the field (S05, Fig.1) using the Ibsen spectroradiometer (Fig. 2).

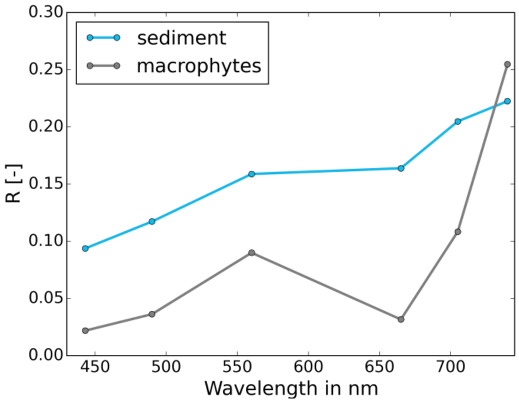

Figure 2. Resampled irradiance reflectance spectra of the two bottom types sediment and macrophytes.

3. RESULTS AND DISCUSSION

3.1. Atmospheric correction

During atmospheric correction Sen2Cor calculated an AOT of 0.218 ± 0.004 (550 nm) for Lake Starnberg pixels. Water vapour above water pixels corresponds to the scene mean above land. Water vapour was 1.42 ±0.14 cm for pixels within a 9x9 km land area surrounding the southern end. Atmospherically corrected spectra showed reasonable magnitudes and shapes of water spectra. Some concerns, however, remained with water pixels. $R_{rs}(0^+)$ values of band B1 (443 nm) showed a constant value of 0.001 sr^{-1} over water surfaces. Furthermore, 12909 pixels showed no data values in band B6 (740 nm) and/or B7 (783 nm). These pixels are located close to the shoreline in the southern part of Lake Starnberg and presumably resulted from overcorrected reflectance (negative values).
Fig. 3 presents in situ and Sen2Cor $R_{rs}(0^+)$ spectra of measurement points. Owing to the no-data issue most measurement points included $R_{rs}(0^+)$ up to 705 nm. High R values (> 0.8) and RMSE values lower than 0.006 sr^{-1} underpinned a good agreement in both shape and magnitude of atmospherically corrected spectra. Absolute $R_{rs}(0^+)$ values varied depending on substrate and water depth. At all measurement points Sen2Cor retrieved lower $R_{rs}(0^+)$ values compared to in situ measurements. This overcorrection may result from an erroneous aerosol parameterization. Sen2Cor estimated a higher aerosol optical thickness compared to microtops measurements (AOT=0.145 (550 nm), cf. [21]). At point S02 which is located very close to the shoreline, Sen2Cor overcorrected $R_{rs}(0^+)$ in all bands.

3.2. Optically deep water

In optically deep water, $a_{CDOM(440)}$, SPM and the sun glint factor g_{dd} were fitted during inverse modelling. Fig. 4 illustrates the resulting constituent maps: they clearly demonstrate that no processing artefacts such as striping close to masked pixels occurred [5]. Low residuals (mean: 2.06E-4 ±1.23E-4 sr^{-1}) between measured S-2A and inversely modelled spectrum further indicated well working modelling. The average SPM concentration was 2.9 ±0.4 mgl^{-1}; average $a_{CDOM(440)}$ was 0.51 ±0.09 m^{-1}. Value ranges of both SPM and $a_{CDOM(440)}$ were reasonable and corresponded well to in situ measurements and concentrations retrieved from remote sensing data from other studies at Lake Starnberg (e.g. [5], [6]).
Referring to the spatial patterns of water constituents, SPM exhibited only small variations (Fig. 4). Lowest SPM values appeared in the northern part, east of the small island 'Roseninsel'. Slightly higher concentrations occurred in the southern part close to shallow waters. CDOM originates from decaying algae and plants or enters the lake from allochthonous sources [22]. Water samples revealed very low concentrations of chl-a (0.6 ±0.2 µgL^{-1}). Therefore, the present CDOM presumably originates from allochthonous inputs. Only small surface waters flow into the lake. Thus, the retrieved low $a_{CDOM(440)}$ values were reasonable; the same applies for highest $a_{CDOM(440)}$ absorption which occurred in the southern part close to the major inflow; accordingly lowest absorption was in the centre of the lake. The sun glint factor g_{dd} ranged between -0.1 and 0.2 (mean: 0.09 ± 0.06). Positive values indicating a proportion of sun glint mainly occurred in the centre and northern part of the lake (Fig. 4). Negative values were fitted in the southern part close to shallow water, which further indicates an overcorrected atmospheric scattering.
Tab. 2 compares WASI derived concentrations with water sample measurements. Although obtained SPM concentrations were in a reasonable range, WASI 2D overestimated SPM concentrations from S-2A data in comparison to analyzed water samples. Certainly, in situ sampling and S-2A acquisition had a time offset of one day; weather conditions, however, were stable and did not indicate changing water constituent concentrations. SPM measurements contain uncertainties [23] which may lead to differences between sample measurements and WASI-2D derived values.

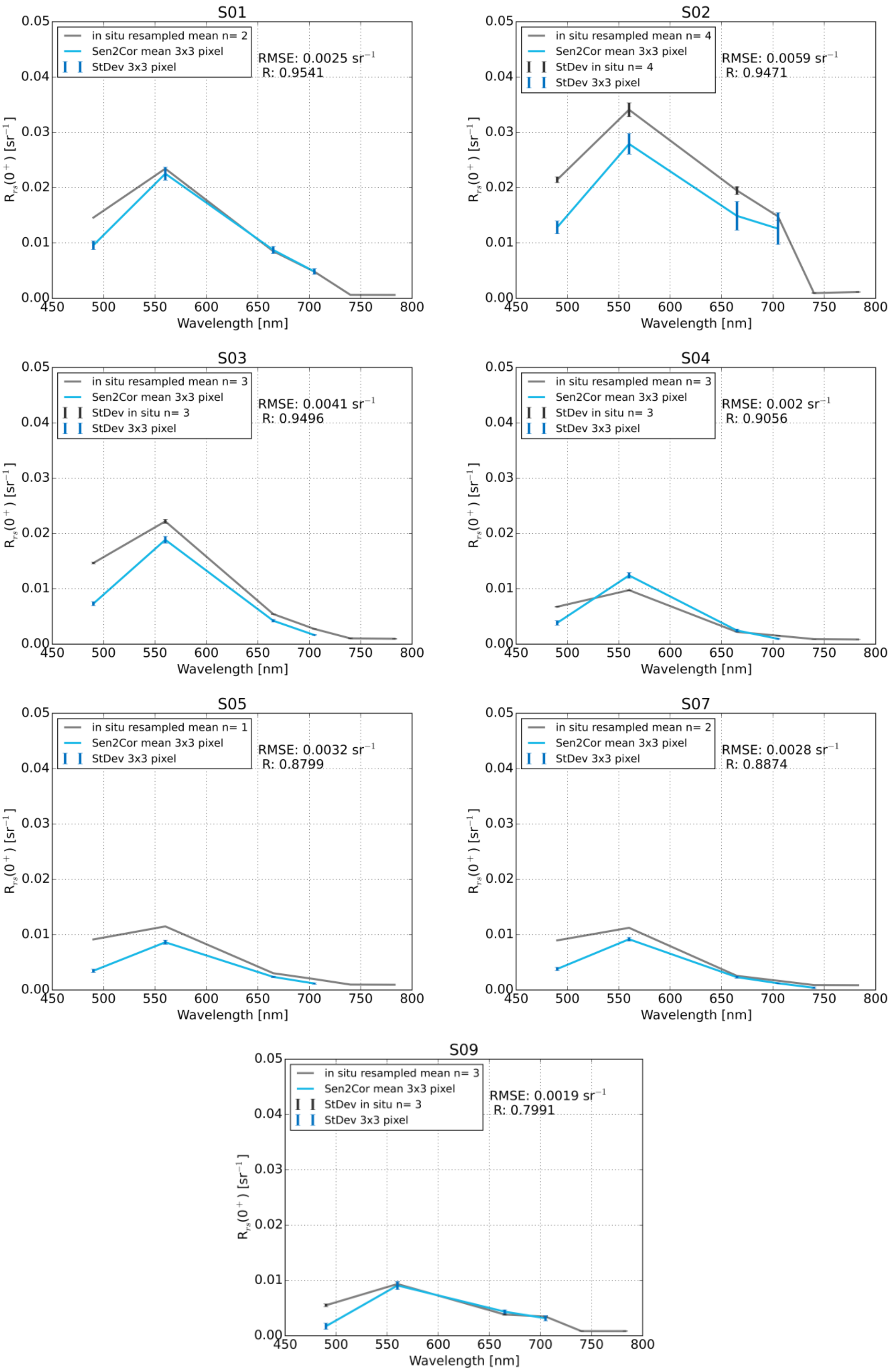

Figure 3. Comparison between resampled in situ measured $R_{rs}(0^+)$ spectra and atmospheric corrected S-2A spectra. S01-S04 and S09 are located in optically shallow water; S05 and S07 are located in optically deep water. At S06 and S10 no measurements were conducted.

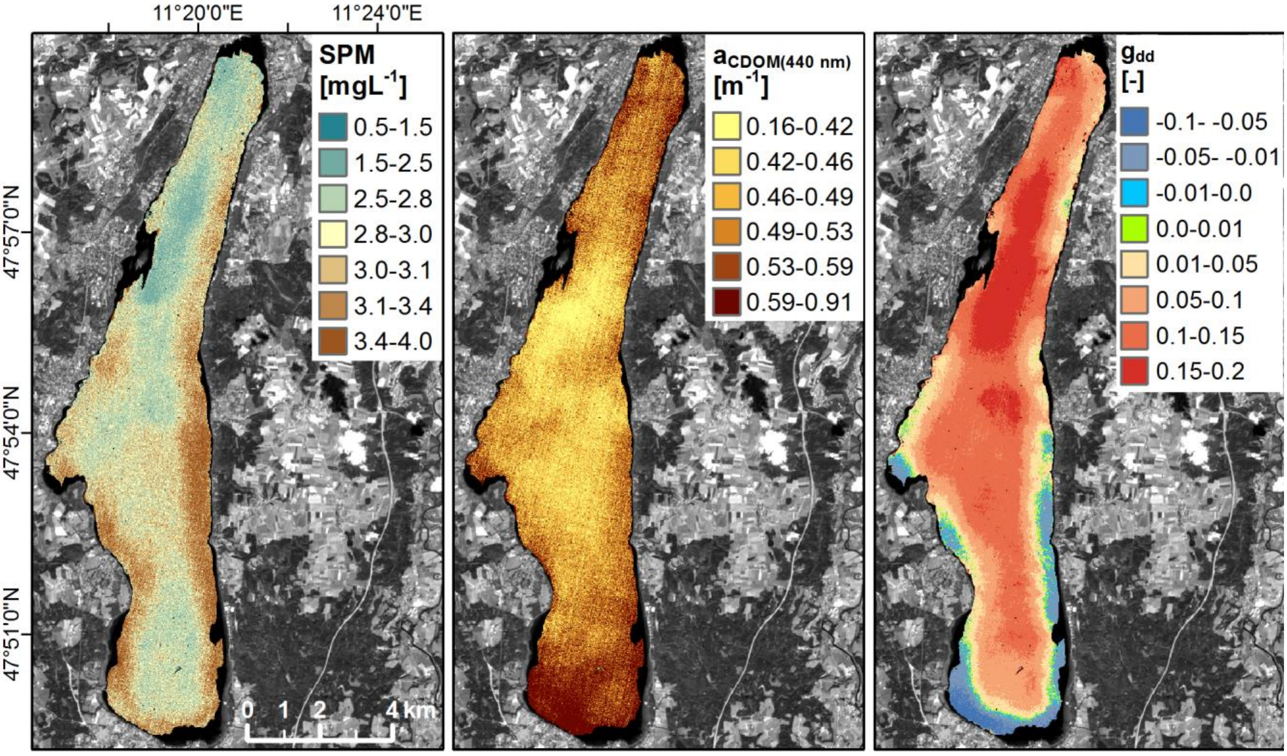

Figure 4. Results of deep water inversion. Background is grayscaled S-2A band B5 (705 nm).

As backscattering of SPM was parameterized according to the default settings of WASI, the results may be improved by determining site specific backscattering coefficients.

Modelled and measured $a_{CDOM(440)}$ values agreed very well. Nevertheless, the measured $a_{CDOM(440)}$ values may be slightly biased by the used filter of 0.7 µm pore size. The standard pore size to measure a_{CDOM} from a water sample ranges between 0.2 and 0.45 µm ([22],[24],[25]).

Table 2. Comparison between in situ and S-2A (WASI-2D) results in optically deep water.

	S05	**S06**	**S07**	**Mean**
SPM [mgL^{-1}] in situ	1.9	1.0	0.4	1.1
SPM [mgL^{-1}] WASI	3.2	3.4	3.1	3.2
$a_{CDOM(440)}$ [m^{-1}] in situ	0.69	0.66	0.62	0.66
$a_{CDOM(440)}$ [m^{-1}] WASI	0.63	0.73	0.65	0.67

3.3 Optically shallow water

In optically shallow water, retrieval of water depths and bottom coverage by sediment or macrophytes was possible in addition to the water constituents ($a_{CDOM(440)}$ and SPM). Tab. 3 lists measured and modelled water constituent values of the in situ sampling points. Fig. 6 highlights the resulting maps. In some cases, striping occurred close to the deep water mask. Compared to deep water, retrieved SPM concentrations (4.5 ±4.2 mgL^{-1}) and $a_{CDOM(440)}$ (0.71 ±0.32 m^{-1}) were higher in average and showed more variability. Modelled water depths were reasonably and ranged between 0 and 8 m. Only few pixels had water depths > 8 m. Average residuals (3.46E-4 ±5.55E-4) were similarly low as in deep water indicating a good model performance. Retrieved $a_{CDOM(440)}$ was highest in the south (inflow), the north (outlet) and at the shoreline where small creeks drain into the lake. $a_{CDOM(440)}$ measured from samples matched with S-2A derived values; similar to shallow water modelled SPM concentrations were overestimated (Tab. 3). Obtained SPM concentrations were lower in the southern part whereas higher concentrations occurred in the north. A reason may be more intense ship traffic in the north compared to the southern end causing sediment resuspension in shallower water. Most pixels in the southern part contained no data values in bands B6 (740 nm) and B7 (783 nm). Contrary, pixels in the northern part offer $R_{rs}(0^{+})$ which could have been interpreted as scattering by slightly higher SPM values during inversion. A lack of in situ SPM values from measurement point S10 (northern end) impedes a clear explanation. Retrieval of bottom substrates coverage by macrophytes (Fig. 6) was reasonable. Pixels with low macrophyte coverage were detected in areas with predominating sediment, e.g. the narrow strip along the south-eastern shoreline. The sediment spectrum used as a reference for unmixing bottom reflectances during inversion was measured in the southern part. Neither this spectrum nor the spectrum of a single macrophyte species from the WASI database were able to cover the entire range of bottom conditions in the lake. Parameterizing representative and accurate R spectra of bottom substrates, however, is challenging. Several approaches are currently developed such as image based retrieval [5], development of reflectance models from in situ measurements [26] or ex situ measurements [27]. Suitable bottom spectra are essential since they strongly influence accurate water depth retrieval [5].

The derived water depth map (Fig. 6) showed reasonable gradients from shallow water at the shoreline towards higher depths close to the deep water mask. Very shallow water depths surrounding the 'Roseninsel' (blue subset in Fig. 6) were detected well. Retrieving the depth gradient between island and shoreline, however, failed, presumably due to inappropriate bottom reference spectra. The same applied for the northern part of the lake, where water depths rarely exceeded 2 m. For a quantitative accuracy assessment echo sounding data were available for the southern part (Fig. 6, yellow subset, white points) [5]. We calculated the mean of all measurement points within a 20x20 m pixel; standard deviations ranged between 0.001 m and 0.78 m (mean: 0.11 m). Fig. 5 shows the comparison between averaged echo sounding depths and modelled water depths from S-2A data. Overall, the RMSE was high (0.95 m). Major deviations from the 1:1 line occurred in modelled depths >4 m which was slightly lower than the average measured Secchi depth (4.2 m). In this depth range (0-4 m) the RMSE was distinctly lower, i.e. 0.42 m. Referring to the water depth values in Tab. 3, measured and S-2A depths corresponded well (except S04), taking into account a certain variability within a 20 m pixel. S04 is located close to a break-off edge, so that little GPS variations may have led to highly differing values.

Table 3. Comparison between in situ and S-2A results (WASI-2D) in optically shallow water. No water samples were taken at S09.

	S01	S02	S03	S04	S10	Mean
SPM [mgL^{-1}] in situ	0.7	0.6	0.1	0.1	-	0.4
SPM [mgL^{-1}] WASI	0.0	0.0	1.4	1.3	4.0	1.3
$a_{CDOM(440)}$ [m^{-1}] in situ	0.83	0.65	0.59	0.59	1.03	0.74
$a_{CDOM(440)}$ [m^{-1}] WASI	0.81	1.17	0.55	0.66	0.65	0.77
Water depth [m] in situ	1.65	0.86	2.75	3.85	-	-
Water depth [m] WASI	1.32	0.65	2.63	2.5	-	-

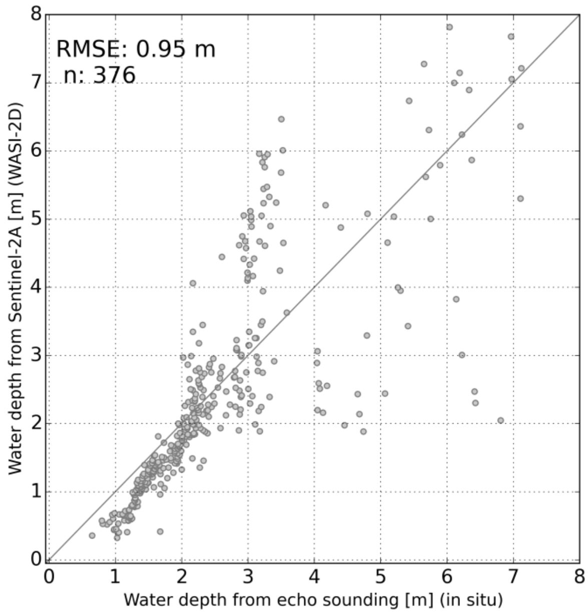

Figure 5. Comparison between echo sounding (acquisition June 2012) and S-2A (WASI-2D) derived water depths.

4. CONCLUSIONS

In this study, we used S-2A data to test its suitability for mapping indicators of lake ecology. To this end, we chose the freely available atmospheric correction tool Sen2Cor and the freely available bio-optical modelling software WASI-2D. We evaluated the performance of the atmospheric correction using in situ $R_{rs}(0^+)$ measurements. Water samples (a_{CDOM}, SPM, chl-a) supported both a regional parameterization of WASI-2D and an assessment of results. In optically deep water, SPM and $a_{CDOM(440)}$ were successfully retrieved from S-2A data. In optically shallow water, SPM and $a_{CDOM(440)}$ could be derived as well as water depth and the presence of bottom macrophyte or sediment. Lacking of S-2A band B1 in the blue impeded chl-a and $a_{CDOM(440)}$ retrieval. The applied atmospheric correction lacks a correction of water surface effects; considering wavelength dependent surface reflectance during WASI-2D inverse modelling, however, allowed the retrieval of reasonable water constituent ranges. In this context, site-specific bottom reflectance spectra proved to be important for obtaining reliable results in optically shallow water.

Overall, S-2A data allowed for gathering spatial information on relevant indicators of lake ecology at Lake Starnberg. Testing its suitability for lake monitoring should be expanded for lakes with differing optical properties and trophic characteristics.

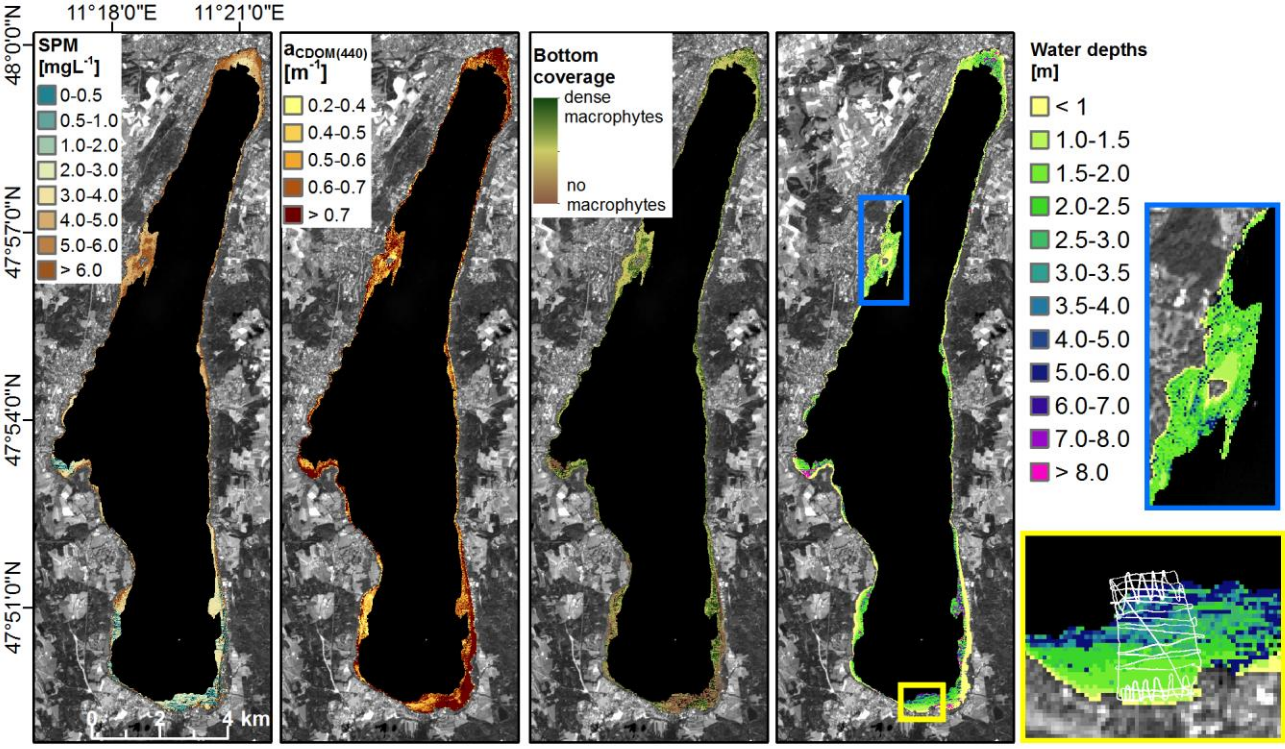

Figure 6. Results of shallow water inversion. Blue subset in water depths map highlights 'Roseninsel', yellow subset depicts validation area with echo sounding track (white points).Background is grayscaled S-2A band B5 (705 nm)

Acknowledgements

This work was conducted within the project LAKESAT (grant no: 50EE1340) funded by the Federal Ministry for Economic Affairs and Energy, Germany. We further thank ESA for providing Sentinel-2A data. We are very grateful to Christine Fritz (TUM), Anna Göritz (DLR), Dr. Markus Hoffmann (TUM), Sebastian Riedel (CAU Kiel) and Dr. Thomas Schneider (TUM) for fieldwork and laboratory analyses.

5. REFERENCES

1. Moss, B. (2012). Cogs in the endless machine: lakes, climate change and nutrient cycles: a review, *Sci. Total Environ.* **434**, 130–142. doi: 10.1016/j.scitotenv.2011.07.069
2. Brönmark, C. & Hansson, L.-A. (2002). Environmental issues in lakes and ponds: current state and perspectives, *Environmental Conservation*. **29**, 290-307. doi: 10.1017/S0376892902000218
3. Birk, S. Bonne, W., Borja, A., Brucet, S., Courrat, A., Poikane, S., Solimini, A., van de Bund, W., Zampoukas, N. & Hering, D. (2012). Three hundred ways to assess Europe's surface waters: An almost complete overview of biological methods to implement the Water Framework Directive, *Ecological Indicators*. **18**, 31–41. doi: 10.1016/j.ecolind.2011.10.009
4. Dörnhöfer, K. & Oppelt, N. (2016). Remote sensing for lake research and monitoring-Recent advances. *Ecological Indicators*. **64**, 105–122. doi:10.1016/j.ecolind.2015.12.009
5. Gege, P. (2014). A case study at Starnberger See for hyperspectral bathymetry mapping using inverse modelling. *Proc. WHISPERS, June 25-27, 2014, Lausanne, Switzerland*
6. Rößler, S., Wolf, P., Schneider, T., Zimmermann, S. & Melzer, A. (2013). Water constituent retrieval and littoral bottom mapping using hyperspectral APEX imagery and submersed artificial surfaces, *EARseL eProceedings*. **12**, 44–57. doi: 10.12760/01-2013-1-05
7. Roessler, S., Wolf, P., Schneider, T. & Melzer, A. (2013). Monitoring of invasive aquatic plants using multitemporal RapidEye-data. In: *Earth Observation of Global Changes (EOGC)*, J. M. Krisp, L. Meng, R. Pail, U. Stilla, Eds. Springer Berlin Heidelberg, pp. 109–123.
8. Müller-Wilm, U. (2016). S2PAD SEN2COR 2.2.0 – Readme, S2PAD-VEGA-SRN-0001.
9. Gege, P. (2014). WASI-2D: A software tool for regionally optimized analysis of imaging spectrometer data from deep and shallow waters, *Computers & Geosciences*. **62**, 208–215. doi: 10.1016/j.cageo.2013.07.022
10. Wöbbecke, K., Klett, G. & Rechenberk, B. (2003). *Wasserbeschaffenheit der wichtigsten Seen in der*

Bundesrepublik Deutschland, *Datensammlung 1981-2000* .

11. BMU (2013). Wasserwirtschaft in Deutschland. Teil 2. Gewässergüte. Bundesministerium für Umwelt, Natuchutz und Reaktorsicherheit (BMU).
12. Gege, P. (2004) Improved Method for Measuring Gelbstoff Absorption Spectra. In: Ocean Optics VXII, CD-ROM. 25-29 October, 2004, Fremantle, Australien.
13. Strömbeck, N., & Pierson, D.C. (2001). The effects of variability in the inherent optical properties on estimations of chlorophyll a by remote sensing in Swedish freshwaters, *Science of The Total Environment*. **268**, 123–137. doi:10.1016/S0048-9697(00)00681-1
14. Sterckx, S., Knaeps, S., Kratzer, S., Ruddick, K. (2015). SIMilarity Environment Correction (SIMEC) applied to MERIS data over inland and coastal waters, *Remote Sensing of Environment*. **157**, 96–110. doi: 10.1016/j.rse.2014.06.017
15. Xu, H. (2006). Modification of normalised difference water index (NDWI) to enhance open water features in remotely sensed imagery, *International Journal of Remote Sensing*. **27**, 3025–3033. doi:10.1080/01431160600589179
16. LfW (2000), Bathymetrie map Lake Starnberg. Landesamt für Wasserwirtschaft Bayern (LfW).
17. IOCCG (2015). Software for Ocean-Colour Data. WASI (Water Colour Simulator), available at: http://www.ioccg.org/data/software.html.
18. Albert, A, & Mobley, C. (2003). An analytical model for subsurface irradiance and remote sensing reflectance in deep and shallow case-2 waters, *Opt. Express*. **11**, 2873. doi:10.1364/OE.11.002873
19. ESA (2015). *Sentinel-2A Spectral Response Functions (S2A-SRF)*.
20. Matthews, M. W. (2011). A current review of empirical procedures of remote sensing in inland and near-coastal transitional waters, *International Journal of Remote Sensing*. **32**, 6855–6899. doi:10.1080/01431161.2010.512947
21. Riedel, S., Gege, P., Pflug, B. & Oppelt, N. (2016). Comparison and evaluation of reflectance spectra and atmospheric parameters derived from HySpex, Sentinel 2A and in-situ measurements of beautiful Bavarian lakes. ESA Living Planet Symposium 2016. Prague, Czech Republic.
22. Brezonik, P. L. , Olmanson, L. G. , Finlay, J. C. & Bauer, M. E. (2015). Factors affecting the measurement of CDOM by remote sensing of optically complex inland waters, *Remote Sensing of Environment*. **157**, 199–215. doi:10.1016/j.rse.2014.04.033
23. Röttgers, R., Heymann, K. & Krasemann, H. (2014). Suspended matter concentrations in coastal waters, *Estuarine, Coastal and Shelf Science*. **151**, 148–155. doi:10.1016/j.ecss.2014.10.010
24. Jiang, G., Ronghua, M., Steven, A. L., Hongtao, D., Wen, S., Weixu, C., Hongtao, D., Yang, J., & Yu, W. (2015). Remote sensing of particulate organic carbon dynamics in a eutrophic lake (Taihu Lake, China), *The Science of The Total Environment*. **532**, 245–254. doi:10.1016/j.scitotenv.2015.05.120
25. Nguy-Robertson, A., Li, L, Tedesco, L. P., Wilson, J. S. & Soyeux, E. (2013). Determination of absorption coefficients for chlorophyll a, phycocyanin, mineral matter and CDOM from three central Indiana reservoirs, *Journal of Great Lakes Research*. **39**, 151–160. doi:10.1016/j.jglr.2013.04.004
26. Fritz, C. & Schneider, T. (2016). Comparing the annual shift of phenologic development of submersed macrophytes based on in situ remote sensing, Poster. ESA Living Planet Symposium 2016. Prague, Czech Republic.
27. Giardino, C., Brescani, M., Valentini, E., Gasperini, L., Bolpagni, R. & Brando, V. E. (2015). Airborne hyperspectral data to assess suspended particulate matter and aquatic vegetation in a shallow and turbid lake, *Remote Sensing of Environment*. **157**, 48–57. doi:10.1016/j.rse.2014.04.034